



ELSEVIER

Optics & Laser Technology 35 (2003) 31–35

Optics & Laser
Technology

www.elsevier.com/locate/optlastec

Fringes of equal tangential inclination by curvature-induced birefringence

M. Medhat^{a,*}, N.I. Hendawy^b, A.A. Zaki^b

^aDepartment of Physics, Faculty of Science, Ain Shams University, Cairo, Egypt

^bDepartment of Physics, Faculty of Science, Benha University, Benha, Kalubia, Egypt

Received 2 January 2002; received in revised form 15 August 2002; accepted 27 August 2002

Abstract

A new kind of interference fringes, fringes of equal tangential inclination by curvature-induced birefringence, is presented. These are two-beam interference fringes produced by bending a thin sheet of birefringent material into a part of an exact cylinder such that the curvature is constant. Due to this curvature there is a uniform birefringence being induced. The change in birefringence induced by applying different radii of curvatures to a Fortepan sheet is measured. The stored (fixed) or natural birefringence of this sheet is deduced. © 2002 Elsevier Science Ltd. All rights reserved.

Keywords: Birefringence; Interference; Photoelasticity

1. Introduction

Photoelasticity is a well-established technique for stress analysis and it has a wide range of industrial and research applications. Several methods of analyzing photoelastic fringe patterns by means of phase-measuring techniques have been presented. Quiroga and Gonzalez Cano [1] presented a phase-measuring algorithm for extraction of the isochromatic of photoelastic fringe patterns. Measurements of birefringence induced in fused-silica specimens by a crack produced by a 351-NM/500-Ps Nd: glass laser was presented [2]. Eugene and Chiayu [3] described a sensitive method for measuring the stress birefringence of an optical window that utilizes a phase-measuring Fizeau interferometer incorporating a visible retarder and a non-polarizing beam splitter. An overdeterministic least-squares phase-stepping method for automated photoelasticity was described [4]. Medhat et al. [5] used an interferometric method to investigate the effect of controlled stress on a transparent plate of plastic. Logan et al. [6] presented measurements of birefringence induced in a suspended sample of fused silica by its suspension. Ye et al. [7] applied

a uniaxial stress to the single crystals of Cr–Cl boracite. The domain structure and the birefringence have been analyzed and correlated to the crystal symmetry of the initial and the induced phase. Gauthier and Farahi [8] studied the effect of externally induced birefringence on visibility and output phase in the optical fiber linking two tandem interferometers. Mivete et al. [9] have studied the interference patterns of multiple reflections from a uniaxial, optically active and non-absorbing plane-parallel plate under oblique incidence. The interference fringes formed by interferometers based on the use of uniaxial wedges were found by Garea and Simon [10]. A method for birefringence measurement using overlapping of interference fringes was developed by Zhaoshu [11]. The present work aims at studying the effect of bending on a polyester base (glossy, retouchable surface) such as Fortepan 200 photographic plate. This effect is investigated both theoretically and experimentally, making use of a new kind of interference fringes. The stored fixed birefringence and induced birefringence for the samples used are evaluated.

2. Theory of fringe formation

When a beam of linearly polarized light emerges from a polarizer and is incident normally on a plane-parallel birefringent crystal plate, of thickness t and having its optic axis

* Corresponding author.

E-mail addresses: mmedhat61@hotmail.com (M. Medhat), hassouba@Yahoo.com (N.I. Hendawy), hassouba@Yahoo.com (A.A. Zaki).

parallel to its surface, it divides into two rays (ordinary and extraordinary) with different velocities of propagation. The light propagates in the same or different directions but with different velocities and this produces a phase shift between the transmitted light waves. The amplitudes of these waves depend on the orientation of their electric vector relative to the optic axis. When the analyzer, which is crossed with the polarizer, recombines the two waves they both acquire equal amplitudes. The regions where the differences of the phases of the waves are even multiples of π appear dark. The regions where the phase differences are odd multiples of π appear bright. The difference in phase φ between the two waves is given by [12]

$$\varphi = (2\pi/\lambda)t|(n_o - n_e)|, \quad (1)$$

where n_o and n_e are the refractive indices in the parallel and perpendicular directions to the optic axis or the applied stress and λ is the wavelength of the light used.

Suppose that a birefringent plate of uniform thickness is placed between two crossed polarizers and illuminated by a parallel beam of monochromatic light normal to it. The plate is uniformly illuminated and the luminous intensity distribution for crossed polarizers is given by [13]

$$I = E^2 \sin^2 \varphi / 2, \quad (2)$$

where E is the amplitude of the light incident on the plate.

It should be noted that if the optic axis is either parallel or perpendicular to the direction of polarization, the fringes will have zero visibility. Also, if the optic axis lies parallel to the direction of propagation, there will be no difference in propagation speeds between the two polarization components, and no fringes are obtained.

Now, if the plate has a variable thickness t , the plate will no longer show uniform illumination and variations of intensity will follow the variations in thickness according to Eq. (1). In a region where one has

$$|(n_o - n_e)|t = q\lambda, \quad (3)$$

the intensity after crossed polarizers will be zero, where q is an integral number, i.e., a dark fringe is observed. Now move to a neighboring region where one has $|(n_o - n_e)|t' = (q + 1)\lambda$; then one observes the next dark fringe. In passing from a dark or bright fringe to the next dark or bright fringe, respectively, the thickness varies by an amount equals to $\lambda/|(n_o - n_e)|$ [14].

In this paper, two-beam interference fringes are produced by bending a thin sheet of transparent photographic film of thickness t into a part of an exact cylinder of constant radius r and center of curvature O as in Fig. 1. Due to this curvature there is a stress applied upon it. This means that two kinds of birefringence are included. One is the stored (fixed) birefringence, which is already present in the sheet and was preimposed into it during its manufacturing. The other is the additional controllable birefringence that is induced on the sample sheet by bending it in a curve, where some stresses are imposed on it. It should be noted

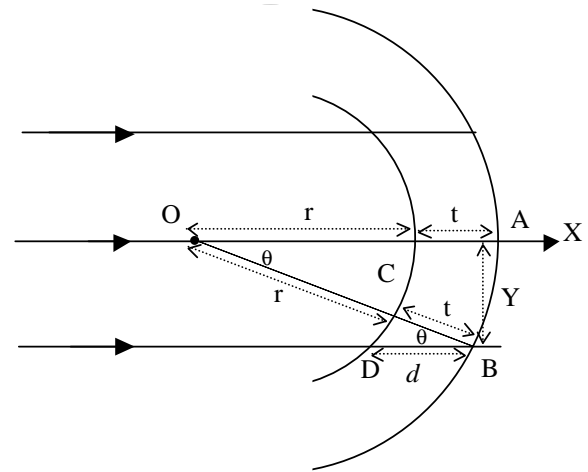


Fig. 1. Transparent anisotropic material in a curved form illuminated with a parallel beam of light.

that bending the film in such a curved manner produces two types of stresses, namely, a compression stress towards the concave face of the film and a tension stress towards the convex face. Thus, the sign of the stress is actually likely to change as it varies from compression to tension through the thickness of the film. These two stresses are not equal and it seems that the strain of the film material due to compression is not equal to that due to tension. The difference between the compression and tension stresses produces a resultant stress that imposes a uniform birefringence all over the film surface. The optic axis lies in the film and takes the shape of its curved surface. In any cross section of the film taken perpendicular to its cylindrical axis, the optic axis is tangent to a circle. It is clear that the optic axis varies in direction rather than lying parallel to a single line. For a collimated light wave, that falls normal to the axis of the film cylinder, the electric vector that is parallel to the cylinder axis is any where perpendicular (vertically) to the optic axis and it contributes to n_o . The electric vector that is perpendicular to the cylinder axis is resolved into two components at the point of incidence on the film. One component is perpendicular to the film surface and hence perpendicular (horizontally) to the optic axis (that contributes also to n_o). The other component is parallel to the film surface and hence parallel to the optic axis at the point of incidence (that contributes to n_e). The stress increases by increasing the curvature of the sheet, i.e., by decreasing the radius of curvature r . Hence, the measured birefringence Δn in presence of stress (through r) is greater than that when no stress is applied, i.e., when $r = \infty$. Therefore, the actual stored birefringence Δn_o is that value corresponding to $1/r = 0$.

A parallel beam of monochromatic light is incident on the concave face of a Fortepan sheet film. Fringes can be seen over relatively wide ranges of both t and r . The relative refraction effects within the film have been neglected because the film is very thin and Δn is small enough. To a

close approximation both faces can be considered to have the same radius of curvature. A geometrical analysis serves to obtain the interference equation as follows. The fringes are formed on a screen behind the sample, perpendicular to the axis of symmetry OX and on both sides of it. Then, the distance between a pair of symmetrically situated fringes on both sides of this axis will be called the diameter of the fringe $2Y$. From Fig. 1 we have

$$\cos \theta \approx (r + t) / \sqrt{(r + t)^2 + Y^2}. \quad (4)$$

Where θ is the angle of incidence and Y is the distance between the situated fringe and the original axis OX which is equal to AB or is the radius of the fringe. But in $\triangle BCD$:

$$\cos \theta \approx t/d, \quad (5)$$

where t is the thickness of the birefringent sample at the center and d is the thickness along the path of the incident parallel beam of light. From Eqs. (4) and (5), we get

$$t/d = (r + t) / \sqrt{(r + t)^2 + Y^2}. \quad (6)$$

Eq. (6) can be rewritten as follows:

$$d = [t/(r + t)] \sqrt{(r + t)^2 + Y^2}. \quad (7)$$

The interference pattern is due to the variation of d which varies with Y . Under this condition the phase difference between the E- and the O-rays is given by Eq. (1). When the phase difference is equal to integral multiples of 2π no light passes through the analyzer, hence, a dark fringe is formed at each thickness for which:

$$\Delta n d = (m + p)\lambda, \quad (8)$$

where $\Delta n = |n_o - n_e|$, m is the order of appearance and p is the order of interference when Y equals zero.

According to Eq. (8), the fringe is the locus of all points of equal Δn and d (or Y). Thus, the fringe shape is a straight line parallel to the cylinder axis. Also, there are two positions on both sides of the axis OX having the same Y and hence the same m . By this means, the fringe pattern is a set of parallel straight lines parallel to the cylinder axis and has a common axis parallel to it and passing by the point $Y = 0$. Around this axis, there are sets of fringes, each has two fringes of the same m and symmetrically placed ($+Y$ and $-Y$) on both sides of this axis. Thus, each fringe although being straight in shape, it has a diameter ($2Y$) and radius Y . Referring to Eq. (4), Y varies with the angle θ , which is the angle between the direction of the incident beam and the radial direction meeting the fringe. Also, from Fig. 1, the angle between the tangent to the sheet at the point of fringe formation (B) and the cord (BA) equals $(\theta/2)$, hence, comes the name fringes of equal tangential inclination

Substituting Eq. (7) into Eq. (8) then,

$$[t/(r + t)] \sqrt{(r + t)^2 + Y^2} = (m + p)\lambda / \Delta n, \quad (9)$$

$$\left[1 + \frac{Y^2}{(r + t)^2} \right]^{1/2} = \frac{m\lambda}{t\Delta n} + \frac{p\lambda}{t\Delta n}. \quad (10)$$

Since $m = 0$ at $Y = 0$ and

$$p = t\Delta n / \lambda,$$

then, substitution in Eq. (10) gives

$$\left[1 + \frac{Y^2}{(r + t)^2} \right]^{1/2} = \frac{m\lambda}{t\Delta n} + 1. \quad (11)$$

By using Maclaurin series the left-hand side of Eq. (11) can be written as follows:

$$\left(1 + \frac{Y^2}{(r + t)^2} \right)^{1/2} = 1 + \frac{1}{2} \frac{Y^2}{(r + t)^2} + \frac{1}{4} \left(\frac{Y^2}{(r + t)^2} \right)^2 + \dots$$

Since $(r + t)^2 \gg Y^2$, then

$$\left(1 + \frac{Y^2}{(r + t)^2} \right)^{1/2} \approx 1 + \frac{1}{2} \frac{Y^2}{(r + t)^2}. \quad (12)$$

By substituting Eq. (12) into Eq. (11) we get

$$1 + \frac{1}{2} \frac{Y^2}{(r + t)^2} = \frac{m\lambda}{t\Delta n} + 1. \quad (13)$$

Then

$$Y^2 = \left[\frac{2\lambda(r + t)^2}{t\Delta n} \right] m. \quad (14)$$

This equation represents a linear relation between the order of the fringe m and the square radius of it Y^2 . There is a direct proportionality between birefringence Δn and the curvature ($1/r$). Also, crowded fringes occur by decreasing the radius of curvature r . By knowing the wavelength of the monochromatic light used, the radius of curvature and thickness t , the induced birefringence Δn is obtained for an anisotropic material.

3. Experimental work and results

The optical setup used to produce two-beam interference fringes in transmission is shown in Fig. 2. O is a mercury lamp with filter ($\lambda = 546.1$ nm) used as a source of light, L_1 is a condensing lens with focal length 3 cm to form minimized image of the source on the pinhole, C is a pinhole to increase the spatial coherence of the light source. L_2 is a collimating lens of focal length 10 cm to produce a parallel beam of light. N_1 is a linear polarizer to give a linearly polarized light. S is the sample of thickness 0.22 mm of developed Fortepan photographic plate in a curved form. This plate is made

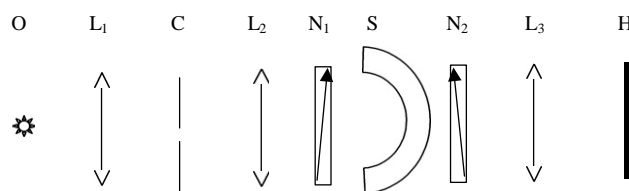


Fig. 2. Optical setup for measuring the birefringence of an anisotropic optical material.

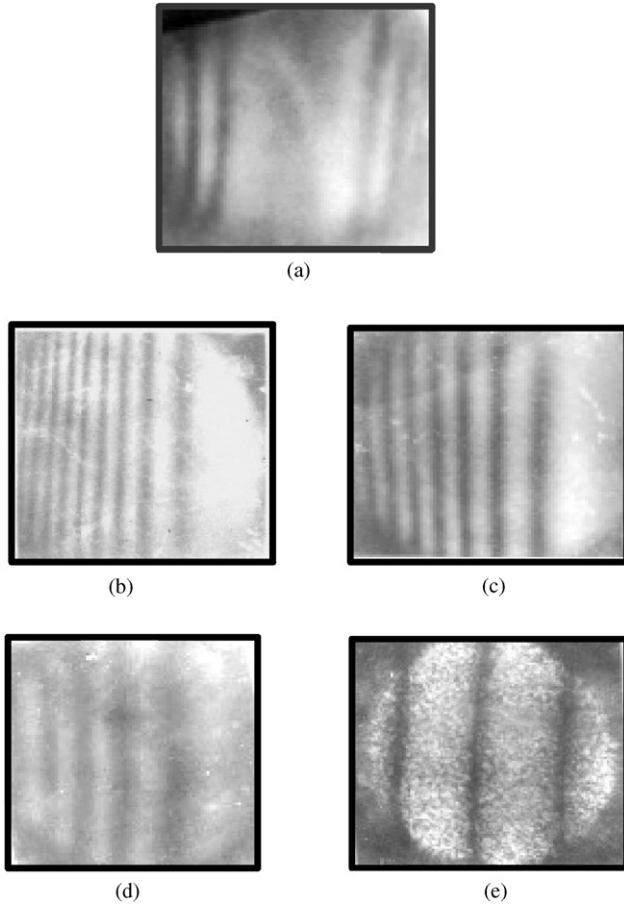


Fig. 3. The interference fringes due to different radii of curvature of Fortepan photographic sheet: (a) fringes around the center ($r = 3$ cm), (b) $r = 2$ cm, (c) $r = 3$ cm, (d) $r = 4$ cm, and (e) $r = 5$ cm.

in Hungary by Forty Photochemical PLC 2601 VAC. N_2 is a linear polarizer placed crossed with N_1 . L_3 is a lens with long focal length 15 cm to form an image on photographic plate H to record the interference pattern. The fringes as recorded on the photographic film H are shown in Fig. 3 for different specified radii of curvature.

The resulting two-beam interference fringes are serially numbered from one to m and their positions on the photographic film are measured. Thus, for each m the value of Y is obtained at a certain radius of curvature. Fig. 4 shows the relation between Y^2 and m at different radii of curvature r (i.e., at different stresses) for the anisotropic sample. From the slopes of these relations Δn is deduced for different specified r .

From the relation between induced birefringence Δn and $1/r$, the value of the natural (stored) birefringence Δn_0 is obtained as shown in Fig. 5. This is the intersection of Δn axis at infinity value of r , i.e., there is no applied stress and the sheet is plane surface. The value of the natural (stored) birefringence (Δn_0) for the sample used is equal to 0.031 for $\lambda = 546.1$ nm.

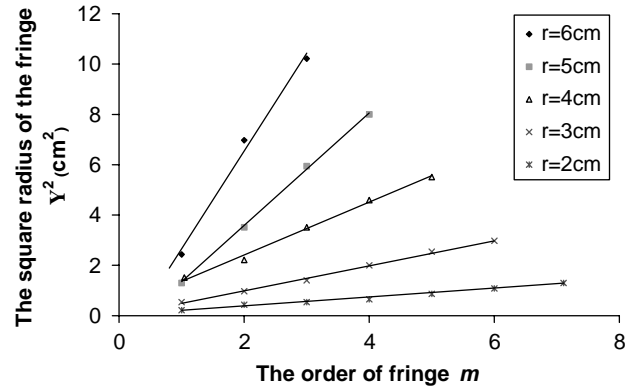


Fig. 4. Relation between squared radius of fringe Y^2 and the order of fringe m at different radii of curvature with a mercury lamp of wavelength 546.1 nm.

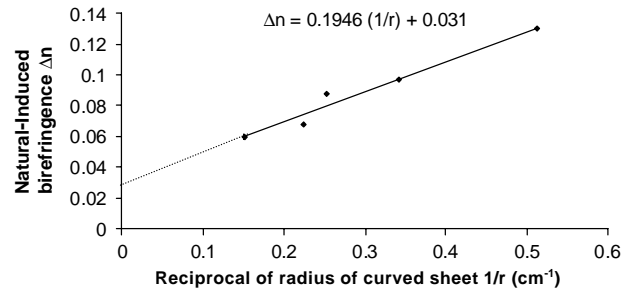


Fig. 5. The relation between induced birefringence Δn for a developed Fortepan transparent photographic plate as an anisotropic material by using a mercury lamp of wavelength equal to 546.1 nm, and reciprocal radius of curvature $1/r$.

4. Conclusion

A new kind of interference fringes is presented and used to evaluate induced and natural birefringence. Bending a birefringent plate (Fortepan photographic plate is used in our experiment) changes its birefringence. In a curved sheet, the induced birefringence Δn at each radius of curvature is obtained. The induced birefringence Δn increases by decreasing radius of curvature (i.e., by increasing the applied stress causing curvature.) and the number of fringes increases and crowds around the center. The natural (stored) birefringence Δn_0 for a Fortepan photographic plate is obtained at infinity value for the radius of curvature (zero stress). The error of finding Δn is found from Eq. (14) as follows:

$$\frac{\delta(\Delta n)}{\Delta n} = \frac{\delta\lambda}{\lambda} + \frac{\delta t}{t} + \frac{2\delta r}{r} + \frac{2\delta Y}{Y} + \frac{\delta m}{m}. \quad (15)$$

The error in $\delta\lambda$ is 10^{-2} nm, $\delta t = 5 \times 10^{-3}$ mm, $\delta r = 5 \times 10^{-2}$ mm and $\delta m = 0$. The error in measuring Y depends on the errors of locating the interference fringe. This error depends on the resolution limit of the reading instrument and the accuracy of locating the peak of the fringe. The resolution of the reading instrument used was 10 μ m, the accuracy of locating the peak depends on its sharpness.

Then $\delta Y = 5 \times 10^{-2}$ mm. For $\lambda = 546.1$ nm, $t = 0.22$ mm, $r = 50$ mm, $Y = 40$ mm and $\Delta n = 0.031$, the error in finding Δn is 8.2×10^{-4} .

References

- [1] Quiroga JA, Gonzalez CA. Appl Opt 1997;36(32):8397.
- [2] Faiz D, Ansgar SW, John LC, Stephen B. Appl Opt 1998;37:33.
- [3] Eugene CR, Chiayu A. Appl Opt 1992;31(31):6702.
- [4] Andrew ND. Appl Opt 1997;36(23):5781.
- [5] Medhat M, El-Zaiat SY, Hindawy SK. Egyptian J Phys 1995;26(1):121.
- [6] Logan JE, Robertson NA, Hough J. Opt Commun 1994;107:342.
- [7] Ye ZG, Burkhardt E, Rivera JP, Schmid H. Ferroelectrics 1995;172:257.
- [8] Gauthier RR, Farahi F. Opt Lett 1994;19(2):138.
- [9] Mivete AI, Lalov II, Wen T, Raptis YS, Anastassakis E. J Phy D 1996;29(10):2705.
- [10] Garea MT, Simon MC. Proc SPIE Int Soc Opt Eng 1996; 2730:220.
- [11] Zhaoshu Liao, Jinguang Tao, Kuntao Tang. Guangxue Jishu Opt Tech 1994;26(1):22.
- [12] Francis JA, Harvey WE. Fundamentals of optics. New York: McGraw-Hill, 1976, p. 546.
- [13] Max B, Emil W. Principles of optics. New York: Pergamon Press, 1980, p. 694.
- [14] Francon M. Optical image formation and processing. London: Academic Press, 1979, p. 10.